

# Action Recognition for Depth Video using Multi-view Dynamic Images

Yang Xiao, Jun Chen, Zhiguo Cao, Joey Tianyi Zhou and Xiang Bai, *Senior Member, IEEE*

**Abstract**—Dynamic image is the recently emerged action representation paradigm able to compactly capture the temporal evolution, especially in context of deep Convolutional Neural Network (CNN). Inspired by its preliminary success towards RGB videos, we propose its extension to the depth domain. To better exploit the 3D characteristics of depth video to leverage the performance, multi-view dynamic image is proposed by us. In particular, the raw depth video will be densely projected onto the different imaging view-points by rotating the virtual camera around the specific instances within the 3D space. Dynamic images are then extracted from the yielded multi-view depth videos respectively to constitute the multi-view dynamic images. In this way, more view-tolerant representative information can be involved in multi-view dynamic images than the single-view counterpart. A novel CNN learning model is consequently proposed to execute feature learning on multi-view dynamic images. The dynamic images from different views will share the same convolutional layers, but with the different fully-connected layers. This model aims to enhance the tuning of shallow convolutional layers by alleviating gradient vanishing. Furthermore, to address the effect of spatial variation an action proposal method based on faster R-CNN is proposed. The dynamic images will be extracted only from the action proposal regions. In experiments, our approach can achieve the state-of-the-art performance on 3 challenging datasets (i.e., NTU RGB-D, Northwestern-UCLA and UWA3DII).

**Index Terms**—action recognition, depth video, multi-view dynamic image, CNN, action proposal

## I. INTRODUCTION

WITH the recently emerged low-cost depth sensors (e.g., Microsoft Kinect [1]), action recognition using depth data is of increasing interest and importance to the fields of video surveillance, multimedia data analysis, human-machine interaction, etc. Compared to the RGB counterpart, depth video can provide richer 3D information to characterize the actions. Numerous of efforts [2]–[9] have already been paid to reveal the effectiveness of 3D representation for action recognition from the different theoretical perspectives. Towards the practical applications, one important research trend is to address the depth-based action recognition problem under the *high intra-class and camera view variation condition, with the large number of action classes*. Some challenging datasets (e.g., NTU RGB-D [10]) have recently been proposed

accordingly. The performance of the existing approaches is unfortunately not satisfactory enough on them. To address this, one feasible way is to seek more discriminative depth-based action representation approach.

To effectively characterize the actions, one of the key issues is to capture the dynamic motion information well. To this end, most of the state-of-the-art RGB-based action recognition approaches [11]–[13] resort to extracting dense optical flow field [14]. For depth video, scene flow [15] is required to reveal the 3D motion characteristics on the other hand. Nevertheless, accurate scene flow estimation is still remaining as a challenging task of high computational burden [16], which is not feasible for the practical applications. An main alternate way to address this is to capture the articulated 3D movement of human body skeleton joints [3], [17], [18]. However, this point-based sparse description paradigm may somewhat lead to information loss. And, the existing human body skeleton extraction methods are still sensitive to pose and imaging viewpoint variation [6], [19]. It may fail to work in cases. Concerning these issues, more concrete motion characterization approach for depth video is required.

Dynamic image [20], [21] is the most recently proposed compact video representation approach, based on the idea of rank pooling [22], [23]. It compresses the video or video clip into a single image, while still maintaining the rich motion information. In context of deep learning technology (i.e., Convolutional Neural Network (CNN) [24]), it has achieved great success for RGB-based action recognition [20], [21], [25] with feasible computational cost. Inspired by this, we propose to extend it to depth domain. To our knowledge, this has not been well studied before. A naive way to this end is to directly apply dynamic image to depth video as the RGB counterpart. However, this cannot fully exploit the 3D motion properties within depth video. To address this, we propose to densely project the raw depth video onto the different imaging view-points by rotating the virtual camera around the specific instances within the 3D space. This procedure is derived from the intrinsic 3D imaging characteristics of depth video, which cannot be achieved on RGB one. Then, dynamic images are extracted from the yielded multi-view depth videos respectively to constitute the multi-view dynamic images for action characterization on motion.

The high adaptability to CNN is one main advantage of dynamic image, which ensures strong discriminative power. In [20], [21], [25], the dynamic images extracted from RGB channels are feed into the one-stream CNN model [26] for action characterization. Here, we argue that this paradigm is not optimal for the proposed multi-view dynamic images on

Yang Xiao, Jun Chen and Zhiguo Cao are with National Key Laboratory of Science and Technology on Multi-Spectral Information Processing, School of Automation, Huazhong University of Science and Technology, P.R. China. E-mail: Yang\_Xiao, chenjun2015, zgcao@hust.edu.cn.

Joey Tianyi Zhou is with Institute of High Performance Computing, A\*STAR, Singapore. E-mail: zhouty@ihpc.a-star.edu.sg.

Xiang Bai is with School of Electronic Information and Communications, Huazhong University of Science and Technology, P.R. China. E-mail: xbai@hust.edu.cn.

Zhiguo Cao is the corresponding author of this paper.

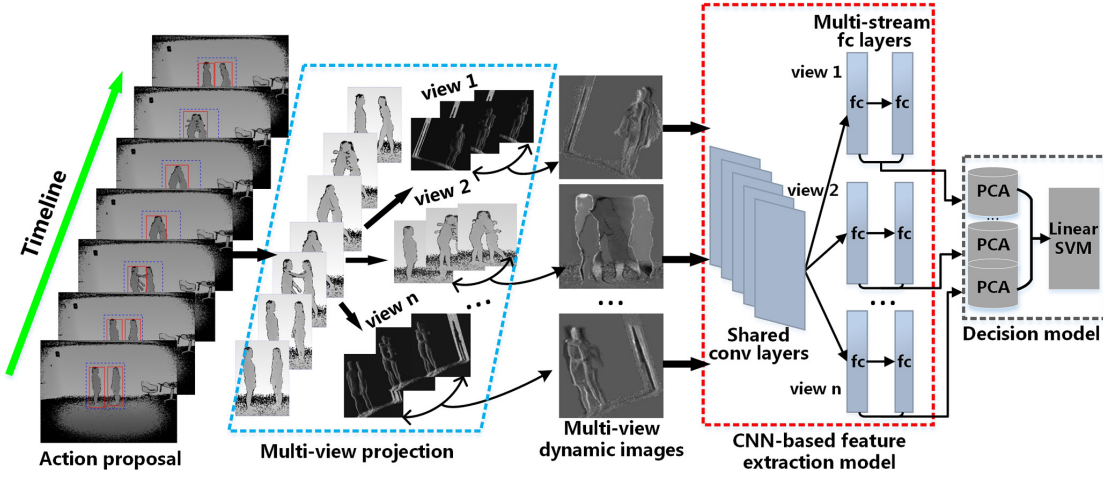


Fig. 1. The main technical pipeline of the proposed action recognition method for depth video using multi-view dynamic images.

depth video. The deep insight is mainly derived from the CNN learning perspective. The problem of gradient vanishing [27], [28] is the critical issue faced by deep neural network training, especially when the training sample amount is limited. It leads to the fact that, the shallow layers (i.e., the convolutional layers) within CNN may not be well tuned [29]. This will weaken the visual pattern capture capacity of CNN. Towards our task, the scale the existing depth action datasets [10], [30], [31] (i.e., 56000 samples at most) is still relative small compared to the large-scale image recognition datasets (e.g., Imagenet [32] of millions samples) fruitful for CNN training. Meanwhile, compared to RGB dynamic images in [20], [21], [25] multi-view dynamic images on depth video are essentially of higher complementary. Hence, our research motivation is to better exploit this complementary property to leverage the training effectiveness on the convolutional layers, in the case that the training samples are not abundant. To this end, a novel CNN learning model is proposed. In particular, the dynamic images from the different virtual imaging view-points will share the same convolutional layers, but correspond to the different fully-connected layers. Towards training, the fully-connected layers of the different view-points will be iteratively tuned. While, the shared convolutional layers are consistently tuned during the whole training phase. In this way, the training error from the different view-points can be back-propagated to the convolutional layers with better chance. Thus, gradient vanishing somewhat can be alleviated. Then, the output of the fully-connected layers will be employed as the visual feature for action recognition with PCA and SVM.

Generally, the actions may happen at the different spatial locations also with the variational scene conditions. Dynamic image is able to fade the background effect, but still spatial-sensitive. This also happens to CNN [33]. To resist the effect of spatial variation, an action proposal method is proposed by us. Specifically, we first employ the state-of-the-art object detector faster R-CNN [34] to detect humans per frame due to its generality and robustness. Then, we merge and link the resulting human detection bounding boxes in the spatial-temporal manner to construct the action proposal volume. It is

worthy noting that, the human-human and human-object interaction information can also be involved in the yielded action proposal volume. Dynamic image is subsequently extracted from the action proposal volume to cope with CNN, not from the whole video. The main technical pipeline our approach is shown in Fig. 1.

The proposed action recognition approach based on multi-view dynamic images is tested on 3 challenging depth datasets (i.e., NTU RGB-D [10], Northwestern-UCLA [31] and UWA3DII [30]). The experimental results demonstrate that, our method can achieve the state-of-the-art performance on all the 3 datasets. The effectiveness of our propositions are also investigated respectively.

The main contributions of this paper are:

- We first extend the concept of dynamic image to depth domain for action recognition. Multi-view dynamic image is proposed to reveal the 3D motion characteristics for action description;
- A novel CNN learning model is proposed to enhance the training performance on multi-view dynamic images;
- An action proposal approach for multi-view dynamic images is proposed to resist the effect of spatial variation.

The source code and supporting materials of this paper will be published upon acceptance.

The remaining of this paper is organized as follows. Sec. II introduces the related work. Sec. III illustrates the concept of multi-view dynamic images in details. The proposed CNN learning model for multi-view dynamic images is given in Sec. IV. The action proposal approach is introduced in Sec. V. Experiments and discussion is conducted in Sec. VI. Sec. VII concludes the whole paper.

## II. RELATED WORK

The depth-based action recognition approaches generally can be categorized into 3 groups: the skeleton-based manner, raw depth video-based manner, and fusion of them.

**Skeleton-based manner.** Under this paradigm, 3D human body skeleton joints [35] are first extracted from the depth frames to characterize the actions. Based on this, Wang *et*

*al.* [2], [3] extracted the spatial-temporal pairwise distance among the skeleton joints as feature, and mined the most discriminative joint combinations for the specific action classes. Vemulapalli *et al.* [18] and Huang *et al.* [36] proposed to extract the discriminative Lie group action representation, from the manifold learning perspective. Weng *et al.* [37] resorted to nearest neighbor search to categorize the actions. A very recent research trend is to capture the spatial-temporal evolution of skeleton joints using recurrent neural network (RNN) [4], [38] or long short term memory network (LSTM) [5], [10], [39]. Although the noticeable progress, skeleton-based manner still suffers from information loss and skeleton joint extraction failure. Meanwhile, CNN cannot intuitively benefit this paradigm to leverage the performance.

**Raw depth video-based manner.** Within this group, the spatial-temporal feature for action description is captured from the raw depth video directly, without extracting the skeletons. Oreifej *et al.* [6] proposed HON4D to characterize the actions by computing the Histogram of Orientated Normal vectors in the 4D space (i.e., XYZ-T). Later, Rahmani *et al.* [40] refined HON4D in the way of encoding Histogram of Oriented Principal Components (HOPC) within the volume around each cloud point. To resist the effect of imaging noise, camera view variation and cluttered background, Lu *et al.* [41] proposed a binary descriptor by executing the pairwise comparison among the 3D cloud points. In [7], the concept of Depth Motion Map (DMM) is proposed to compress the depth video into one single image via aggregating the video frames intuitively by sum pooling. HOG descriptor is consequently extracted on DMM from 3 orthogonal projection planes. Actually, the idea of DMM is somewhat similar to dynamic image. However, it does not involve the temporal evolution characteristics as dynamic image does. HOG was replaced with the FV-encoded LBP in [42]. Wang *et al.* [8], [43] recently applied CNN to DMM, which is similar to our work. The main difference lies 3 folders. First, we verify the superiority of dynamic image over DMM for action characterization in depth video. Secondly, a novel CNN learning model that better copes with multip-view dynamic images is constructed by us. Last, the action proposal procedure is not involved in [8], [43].

**Skeleton and raw depth video fusion manner.** To better use the information from the skeletons and raw depth video Wang *et al.* [44] proposed to extract the Local Occupancy Pattern (LOP) feature from the 3D volume space along the skeleton joints. Following this manner, Yang *et al.* [9] chose to extract Super Normal Vector (SNV) descriptor along the skeleton joints. Althloothi *et al.* [45] and Chaaraoui *et al.* [46] proposed to fuse the skeleton and silhouette shape features.

Our work falls into the second group. Skeleton extraction is not required to ensure the robustness, and involve richer representative information from depth video. To leverage the discriminative power of spatial-temporal feature, dynamic image and CNN model is employed.

### III. MULTI-VIEW DYNAMIC IMAGES

To concretely capture the motion information within depth video, we extend the concept of dynamic image from RGB

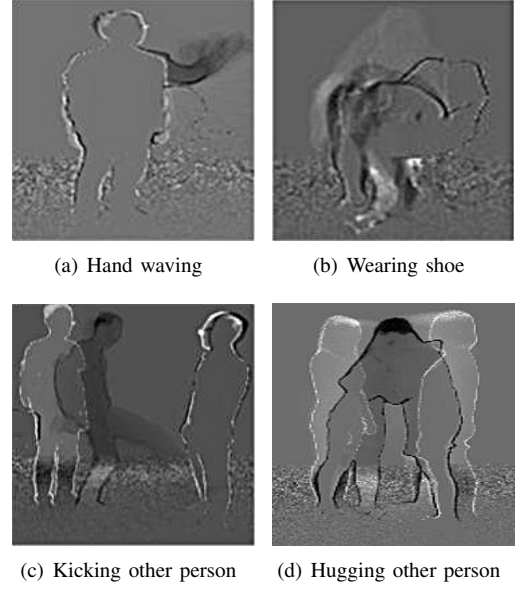


Fig. 2. The dynamic image samples of 4 actions in depth video.

domain to depth domain. By densely projecting the depth video onto multiple virtual imaging points, multi-view dynamic images are consequently extracted to involve more discriminative information. Meanwhile, the training sample amount can be augmented intuitively to better tune CNN.

#### A. Concept of dynamic image

To benefit CNN for action characterization, Bilen *et al.* [20], [21] proposed the concept of dynamic image to capture the spatial-temporal dynamic evolution information within video. One main merit of dynamic images is that, it can summarize the video or video clip into a single static image. Intuitively, this can leverage the efficiency of CNN both for the off-line training and on-line test phases. Suppose  $I_1, \dots, I_T$  denote the video frames, and  $V_t = \frac{1}{t} \times \sum_{i=1}^t I_i$  is the frame average till time  $t$ . Then, a video ranking score function at each time  $t$  is defined as

$$S(t|\mathbf{u}) = \langle \mathbf{u}, V_t \rangle, \quad (1)$$

where  $\mathbf{u} \in \mathbb{R}^d$  is the ranking parameter vector.  $\mathbf{u}$  is learned from the specific video to reflect the ranking relationship among the video frames. The criteria is that, the later frames are associated with the larger ranking scores as

$$q > t \Rightarrow S(q|\mathbf{u}) > S(t|\mathbf{u}). \quad (2)$$

The learning procedure of  $\mathbf{u}$  is consequently formulated as a convex optimization problem based on the framework of RankSVM [47] as

$$\mathbf{u}^* = \underset{\mathbf{u}}{\operatorname{argmin}} \frac{\lambda}{2} \|\mathbf{u}\|^2 + \frac{2}{T(T-2)} \times \sum_{q>t} \max \{0, 1 - S(q|\mathbf{u}) + S(t|\mathbf{u})\}. \quad (3)$$

In particular, the first term is the regularizer usually employed in SVM. And, the second term is the hinge-loss soft-counting



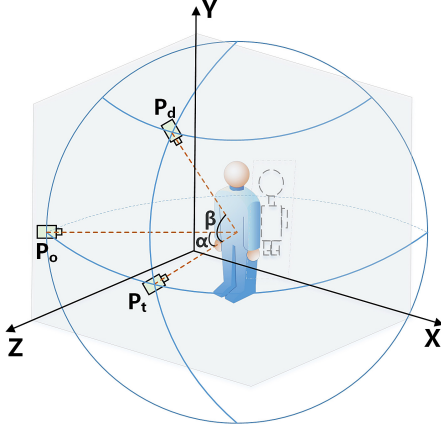


Fig. 3. Rotate the virtual camera within 3D space to mimic the different imaging view-points on depth video.

how many pairs  $q > t$  are incorrectly ranked by the scoring function, which does not meet  $S(q|\mathbf{u}) > S(t|\mathbf{u}) + 1$ . Optimizing Eqn. 3 can map the video frames  $I_i, \dots, I_T$  to a single vector  $\mathbf{u}^*$ . Actually,  $\mathbf{u}^*$  encodes the dynamic evolution information from all the frames. Spatially reordering  $\mathbf{u}^*$  from 1D to 2D can construct dynamic image for video representation. Dynamic image has already demonstrated its superiority for RGB video to characterize action [20], [21], [25]. Here, we find that it can also be extended to depth video. Fig. 2 shows the dynamic image samples of 4 actions (i.e., “hand waving”, “wearing shoe”, “kicking other person”, and “hugging other person”) in the depth videos from NTU RGB-D dataset [10]. It can be observed that, the discriminative dynamic motion information within the video frames can be revealed by one single dynamic image, while suppressing background. Meanwhile, the motion temporal order is also reflected by the gray-scale value.

However, intuitively applying dynamic image to depth domain cannot fully exploit the 3D visual clues contained in depth video. To alleviate this, we propose to densely project the depth video onto multiple virtual imaging points in 3D space. Dynamic images are consequently extracted from the yielded depth videos to construct multi-view dynamic images.

### B. Multi-view projection on depth video

Unlike the RGB counterpart, due to the 3D property depth video can be observed from the different imaging view-points. It can be achieved by rotating the virtual camera around the specific instances in 3D space as shown in Fig. 3. Actually, this is equal to rotate the 3D points within the depth frames. As a consequence, a series of synthesized depth videos can be generated via multi-view projection on the raw one. Indeed, this helps to better mine 3D discriminative visual information and execute data augment for CNN training simultaneously.

As in Fig. 3, suppose we want to move the virtual camera from  $P_o$  to  $P_d$  we can first move  $P_o$  to  $P_t$  with rotation angle  $\alpha$  around  $Y$  axis, and then move  $P_t$  to  $P_d$  with rotation angle  $\beta$  around  $X$  axis. The corresponding 2 rotation matrices for

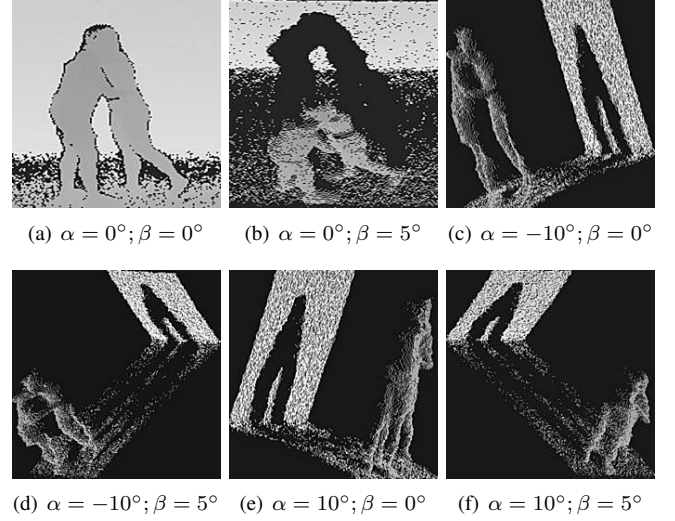


Fig. 4. Some multi-view projection results on depth frame. In particular, “ $\alpha = 0^\circ; \beta = 0^\circ$ ” corresponds to the raw depth frame.

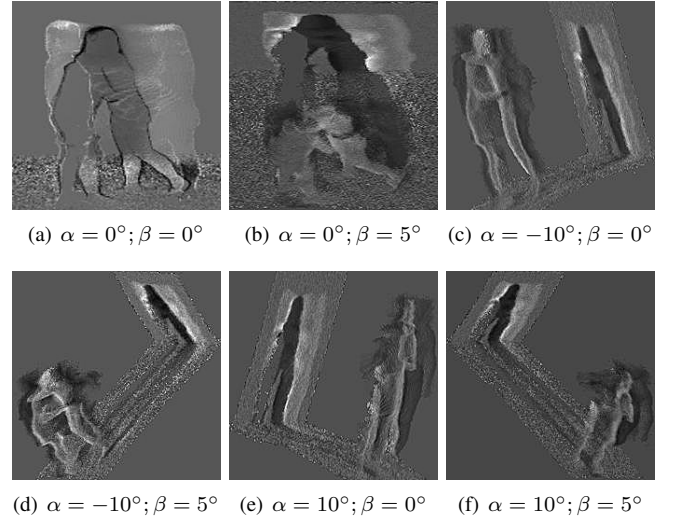


Fig. 5. The dynamic images that correspond to the multi-view projection results in Fig. 4.

3D point coordinate transformation are given by

$$\mathbf{R}_x = \begin{bmatrix} \cos(\beta) & 0 & \sin(\beta) \\ 0 & 1 & 0 \\ -\sin(\beta) & 0 & \cos(\beta) \end{bmatrix}, \quad (4)$$

and

$$\mathbf{R}_y = \begin{bmatrix} 1 & 0 & 0 \\ 0 & \cos(\alpha) & -\sin(\alpha) \\ 0 & \sin(\alpha) & \cos(\alpha) \end{bmatrix}, \quad (5)$$

where the right-handed coordinate system is employed for rotation, and the original camera view-point is regarded as the rotation angle origin. As a consequence, for a 3D point at  $(P_x, P_y, P_z)^T$  after view-point rotation its coordinate will be transferred as

$$(\vec{P}_x, \vec{P}_y, \vec{P}_z)^T = \mathbf{R}_x \mathbf{R}_y (P_x, P_y, P_z)^T, \quad (6)$$

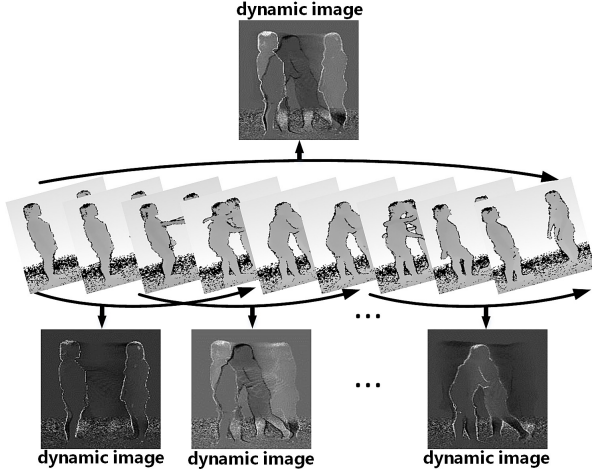


Fig. 6. Temporal split for multi-view dynamic images extraction.

where  $\vec{P}_x$ ,  $\vec{P}_y$  and  $\vec{P}_z$  can be regarded as the new screen coordinates, and the corresponding depth value for the synthesized depth frames. Our multi-view projection approach on depth video is similar to [8], [43]. However, it is worthy noting that our method does not transform  $(P_x, P_y, P_z)^T$  to real-world coordinate system as in [8], [43]. The reason is that, doing this the focal length of depth camera is required, which is not always met in the practical application cases. Thus, our manner is relatively easier and more convenient for application while still ensuring the performance. Fig. 4 shows some multi-view projection results on the specific depth frame, corresponding to different  $\alpha$ - $\beta$  combinations. In particular, “ $\alpha = 0; \beta = 0$ ” corresponds to the raw depth frame. It can be observed intuitively that, more representative visual information is involved in the ensemble of the synthesized depth frames. Meanwhile, the sample amount for the specific action can be significantly enhanced, which helps to alleviate the data-hungry problem during CNN training as aforementioned.

### C. Multi-view dynamic images extraction

After finishing the multi-view projection procedure on depth video, we will consequently extract dynamic images from the synthesized multi-view depth videos (including the raw depth video) individually as shown in Fig. 12. The ensemble of the yielded single-view dynamic images will be termed as multi-view dynamic images for action characterization. Meanwhile, to involve richer temporal information the single-view videos will be split into overlapped segments. The dynamic images will be extracted from the temporal segments and whole single-view video simultaneously as shown in Fig. 6. In particular, each single-view video will be empirically split into 4 temporal segments with the overlap ratio of 0.5. Following [20], [21], the temporal segments share the same action category label as the raw single-view video. Actually, the procedure of temporal split also plays the role of data augment essentially for CNN training to leverage the performance.

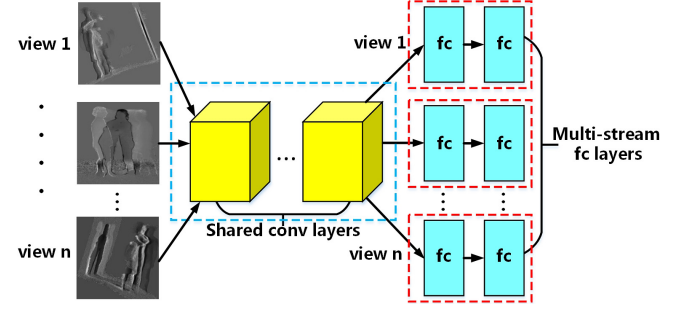


Fig. 7. Multi-view dynamic images adapted CNN learning model.

## IV. MULTI-VIEW DYNAMIC IMAGES ADAPTED CNN LEARNING MODEL

When the multi-view dynamic images have been extracted, they will be fed into CNN for action characterization. Hence, suitable CNN learning model is required to ensure the performance. In our opinion, 2 essential issues should be concerned. First, the scale of the existing depth action datasets [10], [30], [31] (i.e., 56000 samples at most) is still limited, which cannot fully meet the requirement of data-hungry CNN training. Actually, this will aggravate the effect of gradient vanishing problem [27], [28], especially on the shallow convolutional layers that work to capture the visual patterns. Secondly, the multi-view dynamic images are actually of high complementarity as shown in Fig. 12. Nevertheless, the conventional one-stream CNN model [26] employed in [20], [21], [25] cannot reveal this well. In [8], [43], multi-stream CNN model is proposed to alleviate this on multi-view DMMs. That is, the DMMs from different view-points correspond to the individual convolutional and fully-connected layers respectively. However, this model still highly suffers from the training data insufficiency problem. Towards these, our key research motivation is to better exploit the complementary information among the different view-points to benefit CNN training, in the case that the training samples are not abundant.

To this end, a novel multi-view dynamic images adapted CNN learning model is proposed by us as in Fig. 7. In particular, the dynamic images from different view-points share the same convolutional layers (i.e., the same convolutional filters specifically), but correspond to the different fully-connected layers. The intuition is that, the shared convolutional layers work to capture the discriminative fundamental visual patterns among the multi-view dynamic images. While, the multi-stream fully-connected layers aim to reflect the complementarity. During the training phase, the fully-connected layers of the different view-points will be iteratively tuned. While, the shared convolutional layers are consistently trained. Actually, our proposition can somewhat be regarded as the hybrid version of the one-stream CNN model in [20], [21], [25] and the multi-stream model in [8], [43].

The main advantage of our proposition lies in tow-folders. First, compared to the one-stream model in [20], [21], [25], the multi-stream fully-connected layers in our approach help to maintain the complementary information among the view-points. It is worthy noting that, the output of the multi-

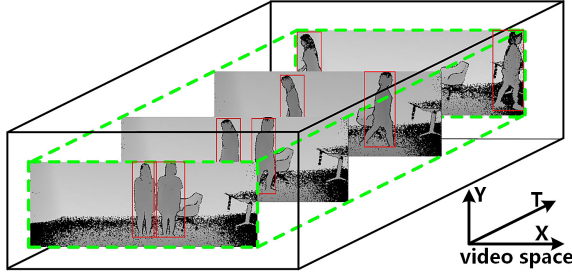


Fig. 8. Action proposal for “walking apart from each other” from NTU RGB-D [10] dataset. In particular, the red bounding boxes are the human detection results using faster R-CNN. And, the green cubic is the action proposal region.

stream fully-connected layers will be concatenated as the visual feature for action recognition with PCA and SVM in our method. On the other hand, compared to the multi-stream model in [8], [43], within our proposition the training error from the different view-points can be back-propagated to the convolutional layers with better chance. Thus, gradient vanishing somewhat can be alleviated, which helps to enhance the training performance on the convolutional layers.

## V. SPATIAL-TEMPORAL ACTION PROPOSAL

In [20], [21], [25], dynamic image extraction is derived from the whole video frames directly. Nevertheless, this is not optimal for the consequent CNN-based visual feature extraction procedure. The reason is that, the actions of the same category may happen at the different spatial locations also with the variational scene conditions. Dynamic image is able to fade the background effect, but still spatial-sensitive. This also happens to CNN [33], especially on the shallow convolutional layers. Indeed, this is unfavourable for stable action representation. As a consequence, effective action proposal is required to alleviate this essential problem.

According to the principal idea that actions are carried out by human [48], a spatial-temporal action proposal approach is proposed by us. In particular, human detection is first executed on each depth frame individually. Then, the resulting human detection bounding boxes are linked and merged in the spatial-temporal manner. That is, the minimal spatial-temporal cubic volume that covers all the bounding boxes closely will be regarded as the action proposal result as shown in Fig. 8. Consequently, the multi-view dynamic images will only be extracted from the yielded action proposal region with some extension<sup>1</sup>, not the whole depth video. Generally, the action items of human-human interaction and human-object interaction can be intrinsically involved in the proposed action proposal approach. Specifically, the off-the-shelf faster R-CNN [34] is employed as our human detector, due to its strong capacity on object detection.

## VI. EXPERIMENTS

In experiments, we will focus on verifying the discriminative power of multi-view dynamic images for action characterization in depth video. 3 challenging action datasets are

<sup>1</sup>Within each frame, the 4 sides of the action proposal bounding box will be extended 30 pixels evenly to involve more discriminative information.

TABLE I  
 $\alpha$ - $\beta$  VIEW GROUP DIVISION, ACCORDING TO THE VALUE OF  $\alpha$ .

View group ( $\beta = 0^\circ$ )	$\alpha$
Group 1	$-90^\circ, -40^\circ$
Group 2	$-20^\circ, -10^\circ, -5^\circ$
Group 3	$0^\circ$
Group 4	$5^\circ, 10^\circ, 20^\circ$
Group 5	$40^\circ, 90^\circ$

employed for test. Specifically, they are NTU RGB-D [10], Northwestern-UCLA [31], and UWA3DII [30]. Although both of the RGB and depth information are involved in these datasets, we only take the depth visual cue into consideration. If not otherwise specified, the available samples in each dataset are split into the training set and testing set according to the original principles in [10], [30], [31].

When executing multi-view projection on depth video, we empirically set  $\beta$  to  $0^\circ$ , and set  $\alpha$  to  $-90^\circ, -40^\circ, -20^\circ, -10^\circ, -5^\circ, 0^\circ, 5^\circ, 10^\circ, 20^\circ, 40^\circ$ , and  $90^\circ$ . It is worthy noting that, the tuple of  $(\alpha = 0^\circ, \beta = 0^\circ)$  corresponds to the raw depth video. Furthermore, the  $\alpha$ - $\beta$  tuples will be divided into 5 view groups as listed in Table I, according to the value of  $\alpha$ . During CNN training, the 5 view groups will share the same convolutional layers, but correspond to the individual fully-connected layers as shown in Fig. 7. The main reason for merging the adjacent  $\alpha$ - $\beta$  tuples into groups is to restrict the CNN model size.

The proposed multi-view dynamic images adapted CNN model is constructed using the CNN-F model [49] that consists of 5 convolutional layers and 3 fully-connected layers. The output of fc7 layer will be employed for action representation. During training, we set most of the training parameters the same as [49] with momentum of 0.9, and weight decay of 0.0005. Nevertheless, in our model the initial learning rate is set to 0.001 decreased by the fact of 10, and batch size is  $8 \times 4$ . The 5 temporal segments of each depth video illustrated in Sec. III-C will be randomly chosen for training (i.e., one for each batch). The training procedure is executed on a single NVIDIA GTX 1080 GPU.

Since the existing faster R-CNN model [34] is generally trained on the RGB object detection datasets, towards human detection in depth video it needs to be re-trained. Thus, sufficient training samples are required. Fortunately, in all the 3 test datasets human body skeleton information is provided per frame. The minimum bounding rectangle that covers all the skeleton joints will be regarded as the ground-truth bounding box of human for training.

LIBLINAR [50] is employed as our SVM classifier. Linear kernel is applied due to efficiency. The penalty factor  $C$  is set via 5-fold cross validation on training set. After PCA, the dimension of feature vector for SVM will be reduced to 1000.

Experimental results are organized as follows. The action recognition results on the 3 benchmark datasets for test is reported in Sec. VI-A to Sec. VI-C. The effectiveness of dynamic image, multi-view projection, multi-view dynamic images adapted CNN model, spatial-temporal action proposal and SVM is demonstrated in Sec. VI-D to VI-H respectively.



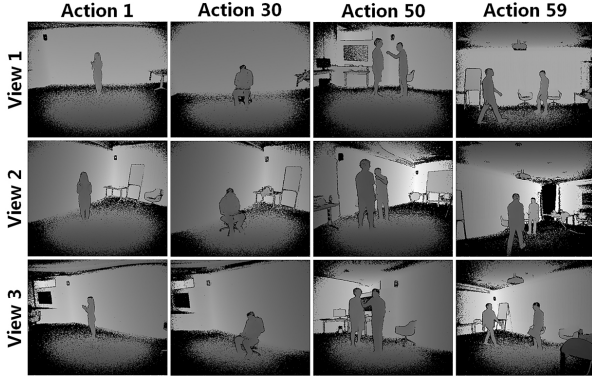


Fig. 9. The key depth frames of 4 actions from 3 different viewpoints in NTU RGB-D dataset.

TABLE II  
PERFORMANCE COMPARISON ON ACTION RECOGNITION ACCURACY (%)  
OF THE DIFFERENT METHODS ON NTU RGB-D DATASET.

Method	Cross-subject	Cross-view
<b>Input: Skeleton data</b>		
Skeletal Quads [51]	38.6	41.4
LARP [18]	50.1	52.8
HBRNN-L [52]	59.1	64.0
FTP Dynamic Skeletons [53]	60.2	65.2
PA-LSTM [10]	63.0	70.3
ST-LSTM [54]	69.2	77.7
GCA-LSTM network [55]	74.4	82.8
Clips+CNN+MTLN [56]	79.6	84.8
<b>Input: Depth maps</b>		
HON4D [6]	30.6	7.3
SNV [9]	31.8	13.6
HOG <sup>2</sup> [57]	32.2	22.3
Multi-view dynamic images+CNN	<b>84.6</b>	<b>87.3</b>

#### A. NTU RGB+D dataset

This is the recently proposed largest-scale dataset for RGB-D human action recognition. In particular, it involves 56000 samples of 60 action classes, which is collected from 40 subjects. The actions can be generally divided into 3 categories: 40 daily actions (*drinking, eating, reading, etc.*), 9 health-related actions (*sneezing, staggering, falling down, etc.*), and 11 mutual actions (*punching, kicking, hugging, etc.*). And, these actions happen under 17 different scene conditions that correspond to 17 video sequences (i.e., S001-S017) respectively. The actions are captured using 3 cameras with the different horizontal imaging viewpoints of  $-45^\circ$ ,  $0^\circ$  and  $+45^\circ$ . Fig. 9 shows some key depth frames of 4 actions in this dataset from 3 different viewpoints. The multi-modality information is provided for action characterization, including depth maps, 3D skeleton joint position, RGB frames, and infrared sequences. The performance evaluation is executed according to 2 principles. One is cross-subject test that splits the 40 subjects into training and test groups. And, the other is cross-view test that employs camera 1 ( $+45^\circ$ ) for test, and the other 2 cameras for training. The performance comparison between our method and the state-of-the-art approaches is listed in Table II. It can be observed that:

- The proposed multi-view dynamic images based action recognition method consistently outperforms all the other

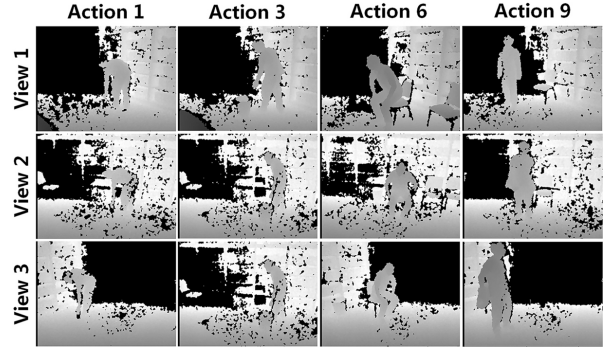


Fig. 10. The key depth frames of 4 actions from 3 different viewpoints in Northwestern-UCLA dataset.

TABLE III  
PERFORMANCE COMPARISON ON ACTION RECOGNITION ACCURACY (%)  
OF THE DIFFERENT METHODS ON NORTHWESTERN-UCLA DATASET.

Method	Accuracy
<b>Input: Skeleton data</b>	
HOJ3D [17]	54.4
Actionlet [3]	69.9
LARP [18]	74.2
<b>Input: Depth maps+human mask</b>	
HPM+TM+external training data [58]	92.0
<b>Input: Depth maps</b>	
CCD [59]	34.4
HON4D [6]	39.9
SNV [9]	42.8
DVV [60]	52.1
AOG [61]	53.6
HOPC [40]	80.0
Multi-view dynamic images+CNN	<b>84.2</b>

state-of-the-art approaches both on the cross-subject and cross-view test settings, disregarding the input is skeleton data or depth maps. This indeed demonstrates the effectiveness of our proposition for depth-based action recognition under the complex scene and imaging viewpoint conditions;

- It is worthy noting that, our method significantly outperforms the other depth maps based approaches by large margins. In our opinion, the essential reason may lie in 3 folders. First, the hand-crafted visual descriptors employed by them is not as discriminative as CNN-based feature learning on multi-view dynamic images in our manner. Secondly, they are sensitive to imaging viewpoint variation. However, in our proposition multi-view projection on depth video can alleviate this. It is noticeable that, our approach can even achieve better performance on cross-view test setting. Last, they take the whole depth maps into consideration for action characterization without effective action proposal. Thus, they are also sensitive to scene and action position variation;

- The skeleton-based approaches achieve much better performance than the depth maps based ones [6], [9], [57], besides our method. And, the most recently proposed depth-based action recognition manners [55], [56] mainly resort to employing skeleton information. However, our proposition verifies the fact that purely using the depth maps can also achieve the comparative or even better performance with the advance of feature learning and human detection.

TABLE IV  
PERFORMANCE COMPARISON ON ACTION RECOGNITION ACCURACY (%) OF THE DIFFERENT METHODS ON UWA3DII DATASET. EACH TIME, 2 VIEWS ARE EMPLOYED FOR TRAINING, AND THE REMAINING 2 VIEWS ARE FOR TEST INDIVIDUALLY.

Training viewpoints	$V_1 \& V_2$		$V_1 \& V_3$		$V_1 \& V_4$		$V_2 \& V_3$		$V_2 \& V_4$		$V_3 \& V_4$		Mean
Test viewpoints	$V_3$	$V_4$	$V_2$	$V_4$	$V_2$	$V_3$	$V_1$	$V_4$	$V_1$	$V_3$	$V_1$	$V_2$	
Input: Skeleton data													
HOJ3D [17]	15.3	28.2	17.3	27.0	14.6	13.4	15.0	12.9	22.1	13.5	20.3	12.7	17.7
Actionlet [3]	45.0	40.4	35.1	36.9	34.7	36.0	49.5	29.3	57.1	35.4	49.0	29.3	39.8
LARP [18]	49.4	42.8	34.6	39.7	38.1	44.8	53.3	33.5	53.6	41.2	56.7	32.6	43.4
Input: Depth maps+human mask													
HPM+TM+external training data [58]	80.6	80.5	75.2	82.0	65.4	72.0	77.3	67.0	83.6	81.0	83.6	74.1	76.9
Input: Depth maps													
CCD [59]	10.5	13.6	10.3	12.8	11.1	8.3	10.0	7.7	13.1	13.0	12.9	10.8	11.2
DVV [60]	23.5	25.9	23.6	26.9	22.3	20.2	22.1	24.5	24.9	23.1	28.3	23.8	24.2
AOG [61]	23.9	31.1	25.3	29.9	22.7	21.9	25.0	20.2	30.5	27.9	30.0	26.8	26.7
HON4D [6]	31.1	23.0	21.9	10.0	36.6	32.6	47.0	22.7	36.6	16.5	41.4	26.8	28.9
SNV [9]	31.9	25.7	23.0	13.1	38.4	34.0	43.3	24.2	36.9	20.3	38.6	29.0	29.9
HOPC [40]	52.7	51.8	59.0	57.5	42.8	44.2	58.1	38.4	63.2	43.8	66.3	48.0	52.2
Multi-view dynamic images+CNN	77.0	59.5	68.3	57.2	57.8	72.9	80.3	51.3	76.6	69.5	78.8	67.9	68.1

### B. Northwestern-UCLA dataset

This dataset contains 1475 video samples of 10 action categories: *pick up with one hand*, *pick up with two hands*, *drop trash*, *walk around*, *sit down*, *stand up*, *donning*, *doffing*, *throw*, and *carry*. They are captured by 3 depth cameras from the different viewpoints with variational scene condition. Each action is executed by 10 subjects. Fig. 10 shows some key depth frames of 4 actions in this dataset from 3 different viewpoints. Compared to NTU RGB-D, the samples in this dataset are of much higher imaging noise, which imposes great challenge to action recognition. The multi-modality information is provided for action characterization, including depth maps, 3D skeleton joint position, and RGB frames. Following [31], the samples from the first 2 cameras are employed for training, and the samples from the 3rd camera are for test. The performance comparison between our approach and the state-of-the-art approaches is listed in Table III. We can summarize that:

- Besides HPM+TM [58], our approach can still achieve better performance than the other state-of-the-art methods when the input is skeleton data or depth maps. It actually verifies the superiority and generality of our proposition on the different datasets;

- The recognition accuracy of HPM+TM method [58] is higher than ours. Nevertheless, it introduces external synthetic data to train CNN. And, accurate human mask is also needed to resist the effect of background and imaging noise. However, our approach does not require these factors. Thus, without external training data our method outperforms all the other manners for comparison;

- It is worthy noting that, the training sample amount of this dataset is much smaller than NTU RGB+D dataset. However, our approach can still achieve good performance (i.e., 84.2%). This demonstrates that, the proposed multi-view dynamic images based action recognition method with CNN is applicable to both of the small-scale and large-scale cases.

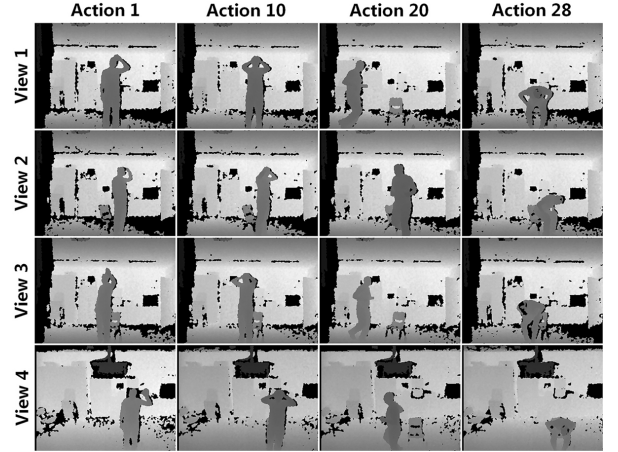


Fig. 11. The key depth frames of 4 actions from 4 different viewpoints in UWA3DII dataset.

### C. UWA3DII dataset

This dataset consists of 1075 action samples from 30 classes: *one hand waving*, *one hand punching*, *two hand waving*, *two hand punching*, *sitting down*, *standing up*, *vibrating*, *falling down*, *holding chest*, *holding head*, *holding back*, *walking*, *irregular walking*, *lying down*, *turning around*, *drinking*, *phone answering*, *bending*, *jumping jack*, *running*, *picking up*, *putting down*, *kicking*, *jumping*, *dancing*, *moping floor*, *sneezing*, *sitting down (chair)*, *squatting*, and *coughing*. These 30 actions are captured from 10 subjects with 4 different imaging viewpoints (i.e., front, top, left, and right), under the same scene condition. The multi-modality information is provided for action characterization, including depth maps, 3D skeleton joint position, and RGB frames. This dataset is challenging mainly due to the issues below. First, the action samples are acquired from the variational viewpoints at the different time points. Secondly, serious self-occlusion may happen. Last but not least, some action categories are of high similarity. Fig. 11 shows some key depth frames of 4 actions in this dataset from 4 different viewpoints. Following [30],



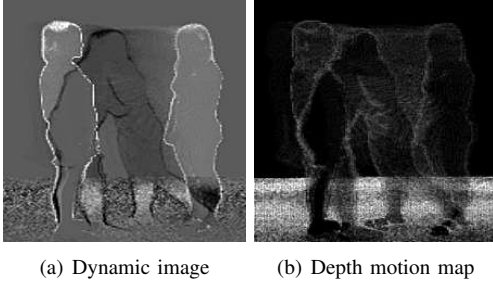


Fig. 12. The dynamic image and depth motion map of “Hugging other person” in NTU RGB-D dataset.

TABLE V  
THE PERFORMANCE COMPARISON ON ACTION RECOGNITION ACCURACY (%) BETWEEN DYNAMIC IMAGE AND DEPTH MOTION MAP (DMM) ON ALL THE 3 TEST DATASETS.

Dataset / Test setting		DMM	Dynamic image
NTU RGB-D	Cross-subject	74.7	<b>84.6</b>
	Cross-view	72.1	<b>87.3</b>
Northwestern-UCLA		78.4	<b>84.2</b>
UWA3D II		51.5	<b>68.1</b>

the samples from 2 imaging viewpoints are employed for training, and the remaining 2 are for test individually. Cross-validation among the viewpoints is executed. The performance comparison between our approach and the state-of-the-art approaches is listed in Table IV. It can be summarized that:

- Corresponding to the different viewpoint combination settings, our method significantly outperforms all the other approaches nearly in all the cases besides HPOC [40] (i.e., training on  $V_1$  &  $V_3$ , and test on  $V_4$ ) and HPM+TM [58]. As aforementioned, HPM+TM employs external training data and human mask. Without considering this, our approach can achieve the best overall performance among all the methods for comparison (i.e., 15.9% better than the second strongest one). Hence, it demonstrates the superiority of our proposition for depth-based action recognition under the more challenging viewpoint variation condition;

- Compared to NTU RGB-D and Northwestern-UCLA dataset, the performance of our approach on this dataset (i.e., overall 68.1%) is relatively low. In our opinion, this may be due to 2 issues. First, the training sample amount of this dataset is not sufficient for CNN training. Secondly, the actions from different categories (e.g., drinking vs. phone answering) are of high similarity. It seems that, dynamic image currently cannot capture and emphasize the fine-grained action characterization clue very well, which should to be addressed in future;

- The performance of skeleton-based methods is indeed poor (i.e., 43.4% at most) on this dataset. This verify the fact that, under the dramatic viewpoint variation and serious self-occlusion conditions accurate action representation using skeleton information is still remaining as a challenging task. As demonstrated by our proposition, using depth maps directly can alleviate this to some degree.

TABLE VI  
THE PERFORMANCE COMPARISON ON ACTION RECOGNITION ACCURACY (%) AMONG VIEW POINT GROUPS IN TABLE I AND THEIR COMBINATION ON S001 SEQUENCE OF NTU RGB-D DATASET.

View group	Cross-subject	Cross-view
Group 1	76.7	75.1
Group 2	78.0	88.4
Group 3	70.4	82.8
Group 4	79.8	91.4
Group 5	78.6	76.5
Group 1+2	80.2	89.5
Group 1+2+3	81.6	93.1
Group 1+2+3+4	84.0	94.3
Group 1+2+3+4+5	<b>84.1</b>	<b>94.9</b>

#### D. Comparison between dynamic image and DMM

As aforementioned, the idea of depth motion map (DMM) [7] is somewhat similar to dynamic image. It can also summarize the depth video into a single image as

$$DMM = \sum_{i=1}^{N-1} (|I_{i+1} - I_i| > \epsilon), \quad (7)$$

where  $I_i$  denotes the  $i$ -th depth frame;  $|I_{i+1} - I_i| > \epsilon$  indicates the binary motion energy map;  $\epsilon$  is the predefined threshold<sup>2</sup>. The intuitive comparison of dynamic image depth motion map is shown in Fig. 12. In particular, they correspond to the same “Hugging other person” action in NTU RGB-D dataset. It can be observed that:

- Dynamic image is able to reveal the motion temporal order of action by the gray-scale value, which cannot be achieved by depth motion map;
- Compared to depth motion map, dynamic image suppresses the effect of background and imaging noise better;
- Due to the unsuitable setting of motion threshold (i.e.,  $\epsilon$  in Eqn. 7), depth motion map tends to loose some action details of relative low motion energy. This is actually detrimental for effective action representation.

Next, we execute the quantitative performance comparison of dynamic image and depth motion map on all the 3 test datasets. In particular, they share the same multi-view projection procedure, CNN learning model, and action proposal results. The performance comparison is listed in Table V. We can observe that, dynamic image significantly outperforms depth motion map in all the test cases. It verifies the superiority of dynamic image for depth video summarization towards action characterization.

#### E. Effectiveness of multi-view projection

To verify the effectiveness of multi-view projection on depth video, we compare the performance of the view groups in Table I and their combination respectively, using the proposed multi-view dynamic images based action recognition method. The test is executed only on S001 action sequence of NTU RGB-D dataset, due to the high computational cost. The performance comparison listed in Table VI. We can see that:

<sup>2</sup>The setting manner of  $\epsilon$  follows [42].

TABLE VII

THE PERFORMANCE COMPARISON ON ACTION RECOGNITION ACCURACY (%) AMONG THE DIFFERENT CNN LEARNING MODEL ON ALL THE 3 TEST DATASETS.

Dataset	OS CNN	MS CNN	Our CNN
NTU RGB-D	78.8	82.5	<b>84.6</b>
Northwestern-UCLA	82.2	82.7	<b>84.2</b>
UWA3DII	57.1	66.4	<b>68.3</b>

- With the increment of view groups, the performance of action recognition is consistently enhanced both on the cross-subject and cross-view test settings. It is worthy noting that, the performance improvement on cross-subject setting demonstrates that multi-view projection on depth video does not only alleviate the cross-view divergence problem but also introduces richer discriminative information for action characterization towards cross-subject case. The results above demonstrate the effectiveness of multi-view projection mechanism on depth video for action recognition;

- As listed in Table I, group 3 corresponds to the raw depth view. However, it is interesting that among all the view groups it does not achieve the best performance. First, this indeed justifies the effectiveness of our view projection method proposed in Sec III-B. Secondly, it reveals the fact that the yielded multi-view projected depth videos do not only play the role of providing additional auxiliary information.

#### F. Effectiveness of multi-view dynamic images adapted CNN learning model

To justify the superiority of the proposed multi-view dynamic images adapted CNN learning model, we compare it with 2 counterparts. One is the multi-stream CNN (MS CNN) learning employed in [8], [43]. That is, the view groups correspond to the individual convolutional and fully-connected layers. And, the other is the standard one-stream CNN (OS CNN) learning model [26]. In particular, the view groups will be regarded as the different input channels. We execute the performance comparison on all the 3 testing datasets with the same experimental settings. On NTU RGB-D dataset, the result on cross-subject test case is reported. The performance comparison is listed in Table VII. It can be summarized that:

- On all the 3 test datasets, the proposed multi-view dynamic images adapted CNN learning model consistently outperforms the other 2 CNN models. This actually demonstrates the effectiveness and generality of our proposition, when coping with multi-view dynamic images for action representation;
- Among all the 3 CNN models, one-stream model is the weakest. The main reason seems that, its structure of only one-stream fc layers is not helpful to capture the complementary information among the different virtual imaging viewpoints.

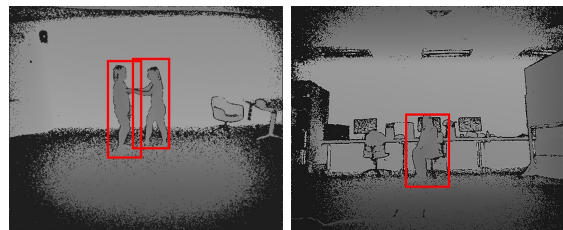
#### G. Effectiveness of spatial-temporal action proposal

In our proposition, spatial-temporal action proposal is executed to resist the effect of scene variation and spatial-sensitivity of CNN. To demonstrate its effectiveness, we compare the test cases with and without action proposal on

TABLE VIII

THE PERFORMANCE COMPARISON ON ACTION RECOGNITION ACCURACY (%) OF THE PROPOSED ACTION RECOGNITION METHOD WITH AND WITHOUT SPATIAL-TEMPORAL ACTION PROPOSAL ON ALL THE 3 TEST DATASETS.

Dataset / Test setting		MVDI-O	MVDI-AP
NTU RGB-D	Cross-subject	78.6	<b>84.6</b>
	Cross-view	75.4	<b>87.3</b>
Northwestern-UCLA		73.2	<b>84.2</b>
UWA3D II		<b>72.6</b>	68.1



(a) Human-human interaction (b) Human-object interaction

Fig. 13. The human detection results of faster R-CNN when human-human or human-object interaction happens.

all the 3 test dataset. The performance comparison is listed in Table VIII. In particular, the proposed multi-view dynamic images based action recognition method with and without action proposal is denoted as “MVDI-AP” and “MVDI-O” respectively. We can see that:

- Action proposal is able to significantly leverage the performance of our method on NTU RGB-D and Northwestern-UCLA datasets in 3 test cases. The performance enhancement is 6.0% at least. This verify the feasibility and effectiveness of our spatial-temporal action proposal approach. This also reveals the fact that, resisting the effect of scene variation and spatial sensitivity of CNN is essential for action recognition;
- On UWA3D II dataset, when action proposal is employed the performance of our approach will unfortunately drop. This may be due to the issue that, the action samples in this dataset are captured under the similar scene condition. Thus, in this case executing action proposal tends to cause information loss. To enhance the adaptability of action proposal is what we plan to address in future.

On the other hand, human detection using faster R-CNN plays the key role for action proposal. We find that, faster R-CNN is highly applicable to depth frames even when human-human or human-object interaction happens. Fig. 13 shows some live examples.

#### H. Comparison between softmax classifier and SVM

In the proposed action recognition approach, SVM is employed as the classifier to decide the action category instead of the softmax classifier in CNN. Our intuition is that, the training sample amount of depth actions is still not sufficient enough to tune CNN well in the end-to-end learning manner. The introduction of SVM can alleviate this. To verify the superiority of SVM, we compare it with softmax classifier on all the 3 test datasets with the same experimental settings and

TABLE IX

THE PERFORMANCE COMPARISON ON ACTION RECOGNITION ACCURACY (%) OF SOFTMAX CLASSIFIER AND SVM ON ALL THE 3 TEST DATASETS.

Dataset / Test setting		Softmax	SVM
NTU RGB-D	Cross-subject	71.8	<b>84.6</b>
	Cross-view	73.7	<b>87.3</b>
Northwestern-UCLA		70.0	<b>84.2</b>
UWA3D II		57.0	<b>68.1</b>

CNN structure. It is worthy noting that, in the proposed CNN model multi-stream softmax classifiers that correspond to the different view groups are involved. Towards softmax-based classification, for a test action sample  $X$  we will fuse the output of the different softmax classifiers by summation to acquire its final classification score. The performance comparison between softmax classifier and SVM is listed in Table IX. It can be summarized that, in all the test cases SVM is significantly better than softmax classifier (i.e., 11.1% better at least). This demonstrates our point that, towards the specific depth-based action recognition task intuitively applying CNN in the end-to-end learning manner but without sufficient training samples is not the optimal choice. Alleviating this according to the idea of unsupervised or low-shot learning on CNN is what we intend to address in future.

## VII. CONCLUSION

In this paper, a novel action recognition approach based on dynamic image for depth video is proposed. Through multi-view projection on depth video, multi-view dynamic images are extracted to characterize the actions by summarize the depth video into static image. The key insight for doing this is involve more discriminative information concerning the 3D property of depth video. To better cope with multi-view dynamic images, a novel CNN learning model is also proposed by us. That is, the different view groups will share the same convolutional layers but with the different fully-connected layers. The main advantage of our CNN model is to alleviate the gradient vanishing problem of CNN training, especially on the shallow convolutional layers. Spatial-temporal action proposal is executed to resist the effect of scene variation and spatial-sensitivity of CNN. The experimental results on 3 test datasets demonstrate the superiority of our approach.

In future work, we plan to study the way that helps to better embed multi-view dynamic images into the deeper CNN structure (i.e., ResNet [29]) by alleviating the high requirement on training sample amount. To enhance the generality of the proposed spatial-temporal action proposal approach for the different scene conditions is also what we concern about.

## REFERENCES

- [1] Zhengyou Zhang. Microsoft kinect sensor and its effect. *IEEE Multimedia*, 19(2):4–10, 2012. 1
- [2] Jiang Wang, Zicheng Liu, Ying Wu, and Junsong Yuan. Mining actionlet ensemble for action recognition with depth cameras. In *Proc. IEEE Conference on Computer Vision and Pattern Recognition (CVPR)*, pages 1290–1297, 2012. 1, 3
- [3] Jiang Wang, Zicheng Liu, and Ying Wu. Learning actionlet ensemble for 3d human action recognition. In *Human Action Recognition with Depth Cameras*, pages 11–40. Springer, 2014. 1, 3, 7, 8
- [4] Vivek Veeriah, Naifan Zhuang, and Guo-Jun Qi. Differential recurrent neural networks for action recognition. In *Proc. IEEE International Conference on Computer Vision (ICCV)*, pages 4041–4049, 2015. 1, 3
- [5] Jun Liu, Gang Wang, Ping Hu, Ling-Yu Duan, and Alex C Kot. Global context-aware attention lstm networks for 3d action recognition. In *Proc. IEEE Conference on Computer Vision and Pattern Recognition (CVPR)*, 2017. 1, 3
- [6] Omar Oreifej and Zicheng Liu. Hon4d: Histogram of oriented 4d normals for activity recognition from depth sequences. In *Proc. IEEE Conference on Computer Vision and Pattern Recognition (CVPR)*, pages 716–723, 2013. 1, 3, 7, 8
- [7] Xiaodong Yang, Chenyang Zhang, and YingLi Tian. Recognizing actions using depth motion maps-based histograms of oriented gradients. In *Proc. ACM International Conference on Multimedia (ACM MM)*, pages 1057–1060, 2012. 1, 3, 9
- [8] Pichao Wang, Wanqing Li, Zhimin Gao, Jing Zhang, Chang Tang, and Philip O Ogunbona. Action recognition from depth maps using deep convolutional neural networks. *IEEE Trans. on Human-Machine Systems*, 46(4):498–509, 2016. 1, 3, 5, 6, 10
- [9] Xiaodong Yang and YingLi Tian. Super normal vector for activity recognition using depth sequences. In *Proc. IEEE Conference on Computer Vision and Pattern Recognition (CVPR)*, pages 804–811, 2014. 1, 3, 7, 8
- [10] Amir Shahroudy, Jun Liu, Tian-Tsong Ng, and Gang Wang. NTU RGB+D: A large scale dataset for 3d human activity analysis. In *Proc. IEEE Conference on Computer Vision and Pattern Recognition (CVPR)*, 2016. 1, 2, 3, 4, 5, 6, 7
- [11] Heng Wang and Cordelia Schmid. Action recognition with improved trajectories. In *Proc. IEEE international Conference on Computer Vision (ICCV)*, pages 3551–3558, 2013. 1
- [12] Karen Simonyan and Andrew Zisserman. Two-stream convolutional networks for action recognition in videos. In *Proc. Advances in Neural Information Processing Systems (NIPS)*, pages 568–576, 2014. 1
- [13] Limin Wang, Yuanjun Xiong, Zhe Wang, Yu Qiao, Dahua Lin, Xiaoou Tang, and Luc Van Gool. Temporal segment networks: Towards good practices for deep action recognition. In *Proc. European Conference on Computer Vision (ECCV)*, pages 20–36, 2016. 1
- [14] Thomas Brox and Jitendra Malik. Large displacement optical flow: descriptor matching in variational motion estimation. *IEEE Trans. on Pattern Analysis and Machine Intelligence*, 33(3):500–513, 2011. 1
- [15] Tali Basha, Yael Moses, and Nahum Kiryati. Multi-view scene flow estimation: A view centered variational approach. *International Journal of Computer Vision*, 101(1):6–21, 2013. 1
- [16] Nikolaus Mayer, Eddy Ilg, Philip Hausser, Philipp Fischer, Daniel Cremers, Alexey Dosovitskiy, and Thomas Brox. A large dataset to train convolutional networks for disparity, optical flow, and scene flow estimation. In *Proc. IEEE Conference on Computer Vision and Pattern Recognition (CVPR)*, pages 4040–4048, 2016. 1
- [17] Lu Xia, Chia-Chih Chen, and J.K. Aggarwal. View invariant human action recognition using histograms of 3d joints. In *Proc. IEEE Conference on Computer Vision and Pattern Recognition Workshops (CVPRW)*, pages 20–27, 2012. 1, 7, 8
- [18] Raviteja Vemulapalli, Felipe Arrate, and Rama Chellappa. Human action recognition by representing 3d skeletons as points in a lie group. In *Proc. IEEE Conference on Computer Vision and Pattern Recognition (CVPR)*, pages 588–595, 2014. 1, 3, 7, 8
- [19] Albert Haque, Boya Peng, Zelun Luo, Alexandre Alahi, Serena Yeung, and Li Fei-Fei. Towards viewpoint invariant 3d human pose estimation. In *Proc. European Conference on Computer Vision (ECCV)*, pages 160–177, 2016. 1
- [20] Hakan Bilen, Basura Fernando, Efstratios Gavves, Andrea Vedaldi, and Stephen Gould. Dynamic image networks for action recognition. In *Proc. IEEE Conference on Computer Vision and Pattern Recognition (CVPR)*, 2016. 1, 2, 3, 4, 5, 6
- [21] Hakan Bilen, Basura Fernando, Efstratios Gavves, and Andrea Vedaldi. Action recognition with dynamic image networks. *arXiv preprint arXiv:1612.00738*, 2016. 1, 2, 3, 4, 5, 6
- [22] Basura Fernando, Efstratios Gavves, Jose M Oramas, Amir Ghodrati, and Tinne Tuytelaars. Modeling video evolution for action recognition. In *Proc. IEEE Conference on Computer Vision and Pattern Recognition (CVPR)*, pages 5378–5387, 2015. 1
- [23] Basura Fernando, Efstratios Gavves, José Oramas, Amir Ghodrati, and Tinne Tuytelaars. Rank pooling for action recognition. *IEEE Trans. on Pattern Analysis and Machine Intelligence*, 39(4):773–787, 2017. 1
- [24] Yann LeCun, Yoshua Bengio, and Geoffrey Hinton. Deep learning. *Nature*, 521(7553):436–444, 2015. 1



- [25] Basura Fernando, Peter Anderson, Marcus Hutter, and Stephen Gould. Discriminative hierarchical rank pooling for activity recognition. In *Proc. IEEE Conference on Computer Vision and Pattern Recognition (CVPR)*, pages 1924–1932, 2016. 1, 2, 4, 5, 6
- [26] Yangqing Jia, Evan Shelhamer, Jeff Donahue, Sergey Karayev, Jonathan Long, Ross Girshick, Sergio Guadarrama, and Trevor Darrell. Caffe: Convolutional architecture for fast feature embedding. In *Proc. ACM International Conference on Multimedia (MM)*, pages 675–678, 2014. 1, 5, 10
- [27] Yoshua Bengio, Patrice Simard, and Paolo Frasconi. Learning long-term dependencies with gradient descent is difficult. *IEEE Trans. on Neural Networks*, 5(2):157–166, 1994. 2, 5
- [28] Xavier Glorot and Yoshua Bengio. Understanding the difficulty of training deep feedforward neural networks. In *Proc. International Conference on Artificial Intelligence and Statistics (AISTATS)*, pages 249–256, 2010. 2, 5
- [29] Kaiming He, Xiangyu Zhang, Shaoqing Ren, and Jian Sun. Deep residual learning for image recognition. In *Proc. IEEE conference on Computer Vision and Pattern Recognition (CVPR)*, pages 770–778, 2016. 2, 11
- [30] Hossein Rahmani, Arif Mahmood, Du Huynh, and Ajmal Mian. Histogram of oriented principal components for cross-view action recognition. *IEEE Trans. on Pattern Analysis and Machine Intelligence*, 38(12):2430–2443, 2016. 2, 5, 6, 8
- [31] Jiang Wang, Xiaohan Nie, Yin Xia, Ying Wu, and Song-Chun Zhu. Cross-view action modeling, learning, and recognition. In *Proc. IEEE Conference on Computer Vision and Pattern Recognition (CVPR)*, pages 2649–2656, 2014. 2, 5, 6, 8
- [32] Jia Deng, Wei Dong, Richard Socher, Li-Jia Li, Kai Li, and Li Fei-Fei. Imagenet: A large-scale hierarchical image database. In *Proc. IEEE Conference on Computer Vision and Pattern Recognition (CVPR)*, pages 248–255, 2009. 2
- [33] Mircea Cimpoi, Subhransu Maji, and Andrea Vedaldi. Deep filter banks for texture recognition and segmentation. In *Proc. IEEE Conference on Computer Vision and Pattern Recognition (CVPR)*, pages 3828–3836, 2015. 2, 6
- [34] Shaoqing Ren, Kaiming He, Ross Girshick, and Jian Sun. Faster R-CNN: Towards real-time object detection with region proposal networks. In *Proc. Advances in Neural Information Processing Systems (NIPS)*, pages 91–99, 2015. 2, 6
- [35] Jamie Shotton, Toby Sharp, Alex Kipman, Andrew Fitzgibbon, Mark Finocchio, Andrew Blake, Mat Cook, and Richard Moore. Real-time human pose recognition in parts from single depth images. *Communications of the ACM*, 56(1):116–124, 2013. 2
- [36] Zhiwu Huang, Chengde Wan, Thomas Probst, and Luc Van Gool. Deep learning on lie groups for skeleton-based action recognition. In *Proc. IEEE Conference on Computer Vision and Pattern Recognition (CVPR)*, 2017. 3
- [37] Junwu Weng, Chaoqun Weng, and Junsong Yuan. Spatio-temporal naive-bayes nearest-neighbor (st-nbnn) for skeleton-based action recognition. In *Proc. IEEE Conference on Computer Vision and Pattern Recognition (CVPR)*, 2017. 3
- [38] Yong Du, Wei Wang, and Liang Wang. Hierarchical recurrent neural network for skeleton based action recognition. In *Proc. IEEE Conference on Computer Vision and Pattern Recognition (CVPR)*, pages 1110–1118, 2015. 3
- [39] Wentao Zhu, Cuiling Lan, Junliang Xing, Wenjun Zeng, Yanghao Li, Li Shen, and Xiaohui Xie. Co-occurrence feature learning for skeleton based action recognition using regularized deep lstm networks. *arXiv preprint arXiv:1603.07772*, 2016. 3
- [40] Hossein Rahmani, Arif Mahmood, Du Q Huynh, and Ajmal Mian. HOPC: Histogram of oriented principal components of 3d pointclouds for action recognition. In *Proc. European Conference on Computer Vision (ECCV)*, pages 742–757, 2014. 3, 7, 8, 9
- [41] Cewu Lu, Jiaya Jia, and Chi-Keung Tang. Range-sample depth feature for action recognition. In *Proc. IEEE Conference on Computer Vision and Pattern Recognition (CVPR)*, pages 772–779, 2014. 3
- [42] Chen Chen, Roozbeh Jafari, and Nasser Kehtarnavaz. Action recognition from depth sequences using depth motion maps-based local binary patterns. In *Proc. IEEE Winter Conference on Applications of Computer Vision (WACV)*, pages 1092–1099. IEEE, 2015. 3, 9
- [43] Pichao Wang, Wanqing Li, Zhimin Gao, Chang Tang, Jing Zhang, and Philip Ogunbona. Convnets-based action recognition from depth maps through virtual cameras and pseudocoloring. In *Proc. ACM International Conference on Multimedia (ACM MM)*, pages 1119–1122, 2015. 3, 5, 6, 10
- [44] Jiang Wang, Zicheng Liu, Jan Chorowski, Zhuoyuan Chen, and Ying Wu. Robust 3d action recognition with random occupancy patterns. In *Proc. European Conference on Computer Vision (ECCV)*, pages 872–885, 2012. 3
- [45] Salah Althloothi, Mohammad H Mahoor, Xiao Zhang, and Richard M Voyles. Human activity recognition using multi-features and multiple kernel learning. *Pattern Recognition*, 47(5):1800–1812, 2014. 3
- [46] Alexandros Chaaaroui, Jose Padilla-Lopez, and Francisco Flórez-Revuelta. Fusion of skeletal and silhouette-based features for human action recognition with rgb-d devices. In *Proc. IEEE International Conference on Computer Vision Workshops (ICCVW)*, pages 91–97, 2013. 3
- [47] Alex J Smola and Bernhard Schölkopf. A tutorial on support vector regression. *Statistics and Computing*, 14(3):199–222, 2004. 3
- [48] Gang Yu and Junsong Yuan. Fast action proposals for human action detection and search. In *Proc. IEEE Conference on Computer Vision and Pattern Recognition (CVPR)*, pages 1302–1311, 2015. 6
- [49] Ken Chatfield, Karen Simonyan, Andrea Vedaldi, and Andrew Zisserman. Return of the devil in the details: Delving deep into convolutional nets. *Proc. British Machine Vision Conference (BMVC)*, 2014. 6
- [50] Rongen Fan, Kaiwei Chang, Chojui Hsieh, Xiangrui Wang, and Chihjen Lin. Liblinear: A library for large linear classification. *Journal of Machine Learning Research*, 9:1871–1874, 2008. 6
- [51] G. Evangelidis, G. Singh, and R. Horaud. Skeletal quads: Human action recognition using joint quadruples. In *International Conference on Pattern Recognition*, pages 4513–4518, 2014. 7
- [52] Yong Du, Wei Wang, and Liang Wang. Hierarchical recurrent neural network for skeleton based action recognition. In *Proc. IEEE Conference on Computer Vision and Pattern Recognition (CVPR)*, pages 1110–1118, 2015. 7
- [53] Jian Fang Hu, Wei Shi Zheng, Jianhuang Lai, and Jianguo Zhang. Jointly learning heterogeneous features for rgb-d activity recognition. In *IEEE Conference on Computer Vision and Pattern Recognition*, pages 5344–5352, 2015. 7
- [54] Jun Liu, Amir Shahroudy, Dong Xu, and Gang Wang. Spatio-temporal lstm with trust gates for 3d human action recognition. In *Proc. European Conference on Computer Vision (ECCV)*, pages 816–833, 2016. 7
- [55] Qihong Ke, Mohammed Bennamoun, Senjian An, Ferdous Sohel, and Farid Boussaid. A new representation of skeleton sequences for 3d action recognition. In *Proc. IEEE Conference on Computer Vision and Pattern Recognition (CVPR)*, 2017. 7
- [56] Jun Liu, Gang Wang, Ping Hu, Ling-Yu Duan, and Alex C Kot. Global context-aware attention lstm networks for 3d action recognition. In *Proc. IEEE Conference on Computer Vision and Pattern Recognition (CVPR)*, 2017. 7
- [57] E. Ohn-Bar and M. M. Trivedi. Joint angles similarities and HOG2 for action recognition. In *Proc. IEEE Conference on Computer Vision and Pattern Recognition Workshops (CVPRW)*, pages 465–470, 2013. 7
- [58] Hossein Rahmani and Ajmal Mian. 3D action recognition from novel viewpoints. In *Proc. IEEE Conference on Computer Vision and Pattern Recognition (CVPR)*, 2016. 7, 8, 9
- [59] Zhongwei Cheng, Lei Qin, Yituo Ye, Qingming Huang, and Qi Tian. Human daily action analysis with multi-view and color-depth data. In *Proc. International Conference on Computer Vision (ICCV)*, pages 52–61, 2012. 7, 8
- [60] Ruonan Li and T. Zickler. Discriminative virtual views for cross-view action recognition. In *Proc. IEEE Conference on Computer Vision and Pattern Recognition (CVPR)*, pages 2855–2862, 2012. 7, 8
- [61] Jiang Wang, Xiaohan Nie, Yin Xia, and Ying Wu. Cross-view action modeling, learning, and recognition. In *Proc. IEEE Conference on Computer Vision and Pattern Recognition (CVPR)*, pages 2649–2656, 2014. 7, 8